

FINITE ENERGY CHIRAL SUM RULES
AND τ SPECTRAL FUNCTIONSM. Davier^{a,1}, L. Girlanda^{b,2}, A. Höcker^{a,3} and J. Stern^{b,4}^a*Laboratoire de l'Accélérateur Linéaire,
IN2P3-CNRS et Université de Paris-Sud, F-91405 Orsay, France*^b*Division de Physique Théorique, Institut de Physique Nucléaire
Université de Paris-Sud, F-91406 Orsay, France***Abstract**

A combination of finite energy sum rule techniques and Chiral Perturbation Theory (χ PT) is used in order to exploit recent ALEPH data on the non-strange τ vector (V) and axial-vector (A) spectral functions with respect to an experimental determination of the χ PT quantity L_{10} . A constrained fit of $R_{\tau,V-A}^{(k,l)}$ inverse moments ($l < 0$) and positive spectral moments ($l \geq 0$) adjusts simultaneously L_{10} and the nonperturbative power terms of the Operator Product Expansion. We give explicit formulae for the first $k = 0, 1$ and $l = -1, -2$ strange and non-strange inverse moment chiral sum rules to one-loop order generalized χ PT. Our final result reads $L_{10}^r(M_\rho) = -(5.13 \pm 0.19) \times 10^{-3}$, where the error includes experimental and theoretical uncertainties.

*(Submitted to Physics Letters B)*¹E-mail: davier@lal.in2p3.fr²E-mail: girlanda@ipno.in2p3.fr³E-mail: hoecker@lal.in2p3.fr⁴E-mail: stern@ipno.in2p3.fr

1 Introduction

The nonperturbative features of strong interactions make QCD a rich environment for theoretical investigations. At sufficiently high energies it is possible to parametrize the nonperturbative effects by vacuum condensates, following the rules of Wilson's Operator Product Expansion (OPE) [1]. The universal character of these condensates has been used in the derivation of the so-called QCD spectral sum rules [2] allowing, in principle, their determination from experiment. A particular role is played by the condensates which are order parameters of the spontaneous breakdown of chiral symmetry (SB χ S). The latter vanish at all orders of perturbation theory and they control the high energy behavior of chiral correlation functions, such as the difference of vector and axial current two-point functions. On the other hand, at low energies, SB χ S makes it possible to construct an effective theory of QCD, the Chiral Perturbation Theory (χ PT) [3, 4], which uses the Goldstone bosons as fundamental fields and provides a systematic expansion of QCD correlation functions in powers of momenta and quark masses. All missing information is then parametrized by low-energy coupling constants, which can be determined phenomenologically in low-energy experiments involving pions and kaons. The fundamental parameters describing chiral symmetry breaking, the running quark masses and the quark anti-quark condensates $\langle\bar{q}q\rangle$ appear both in low-energy (χ PT) and the high energy OPE expansion. For this reason it is useful to combine the two expansions in order to get a truly systematic approach to the chiral sum rules [5]. In this paper the combined approach is illustrated through a determination of the L_{10} constant of the chiral lagrangian, including high-energy corrections coming from the OPE. The connection between the two domains is provided by experimental data on τ hadronic spectral functions published recently by the ALEPH Collaboration [6, 7].

At the leading order of χ PT, L_{10} is directly linked to the vector, v_1 , and axial-vector, a_1 , spin-one spectral functions (the subscripts refer to the spin J of the hadronic system) through the Das-Mathur-Okubo sum rule [8]

$$\frac{1}{4\pi^2} \int_0^{s_0 \rightarrow \infty} ds \frac{1}{s} [v_1(s) - a_1(s)] \simeq -4L_{10} . \quad (1)$$

As it stands the DMO sum rule (1) is subject to chiral corrections due to non-vanishing quark masses [9]. On the other hand, the integral has to be cut at some finite energy $s_0 \leq M_\tau^2$, since no experimental information on $v_1 - a_1$ is available above M_τ^2 . This truncation introduces an error which competes with the low-energy chiral corrections. Both types of corrections can be systematically included through *i*) the high-energy expansion in $\alpha_s(s_0)$ and in inverse powers of s_0 , and *ii*) the low-energy expansion in powers of quark masses and of their logarithms.

2 Spectral Moments

Using unitarity and analyticity, the spectral functions are connected to the imaginary part of the two-point correlation functions,

$$\begin{aligned}\Pi_{ij,U}^{\mu\nu}(q) &\equiv i \int d^4x e^{iqx} \langle 0 | T(U_{ij}^\mu(x) U_{ij}^\nu(0)^\dagger) | 0 \rangle \\ &= (-g^{\mu\nu} q^2 + q^\mu q^\nu) \Pi_{ij,U}^{(1)}(q^2) + q^\mu q^\nu \Pi_{ij,U}^{(0)}(q^2),\end{aligned}\quad (2)$$

of vector ($U_{ij}^\mu \equiv V_{ij}^\mu = \bar{q}_j \gamma^\mu q_i$) or axial-vector ($U_{ij}^\mu \equiv A_{ij}^\mu = \bar{q}_j \gamma^\mu \gamma_5 q_i$) colour-singlet quark currents for time-like momentum-squared $q^2 > 0$. Lorentz decomposition is used to separate the correlation function into its $J = 1$ and $J = 0$ parts. The correlation function (2) is analytic everywhere in the complex s plane except on the positive real axis where singularities exist. Using the definitions adopted in Refs. [6, 7] together with Eq. (2), one identifies for non-strange quark currents

$$\text{Im} \Pi_{\bar{u}d,V/A}^{(1)}(s) = \frac{1}{2\pi} v_1/a_1(s), \quad \text{Im} \Pi_{\bar{u}d,A}^{(0)}(s) = \frac{1}{2\pi} a_0(s). \quad (3)$$

Due to the conserved vector current, there is no $J = 0$ contribution to the vector spectral function, while the only contribution to a_0 is assumed to be from the pion pole. It is connected via PCAC to the pion decay constant, $a_{0,\pi}(s) = 4\pi^2 f_\pi^2 \delta(s - m_\pi^2)$.

According to the method proposed by Le Diberder and Pich [10], it is possible to exploit the information from the explicit shape of the spectral functions by calculating so-called spectral moments, *i.e.*, weighted integrals over the spectral functions. If $W(s)$ is an analytic function, by Cauchy's theorem, the imaginary part of $\Pi_{ij,V/A}^{(J)}$ is proportional to the discontinuity across the positive real axis:

$$\int_0^{s_0} ds W(s) \text{Im} \Pi_{ij,V/A}^{(J)}(s) = -\frac{1}{2i} \oint_{|s|=s_0} ds W(s) \Pi_{ij,V/A}^{(J)}(s), \quad (4)$$

where s_0 is large enough for the OPE series to converge. The authors of [10] choose for $W(s)$ the functions

$$W^{(k,l)}(s) = \left(1 - \frac{s}{s_0}\right)^{2+k} \left(\frac{s}{s_0}\right)^l, \quad (5)$$

with k and l positive integers. The factor $(1 - s/s_0)^k$ suppresses the integrand at the crossing of the positive real axis where the validity of the OPE is questioned. Its counterpart $(s/s_0)^l$ projects on higher energies. These moments were successfully applied in order to constrain nonperturbative contributions to the τ hadronic width, R_τ , a procedure which lead to precise determinations of $\alpha_s(M_\tau^2)$ [7, 11, 12].

The extension of the spectral moment analysis to negative integer values of l ("inverse moment sum rules", (IMSR) [13]) requires, due to the pole at $s = 0$, a modified contour of integration in the complex s plane, as shown in Fig. 1. This is where χ PT

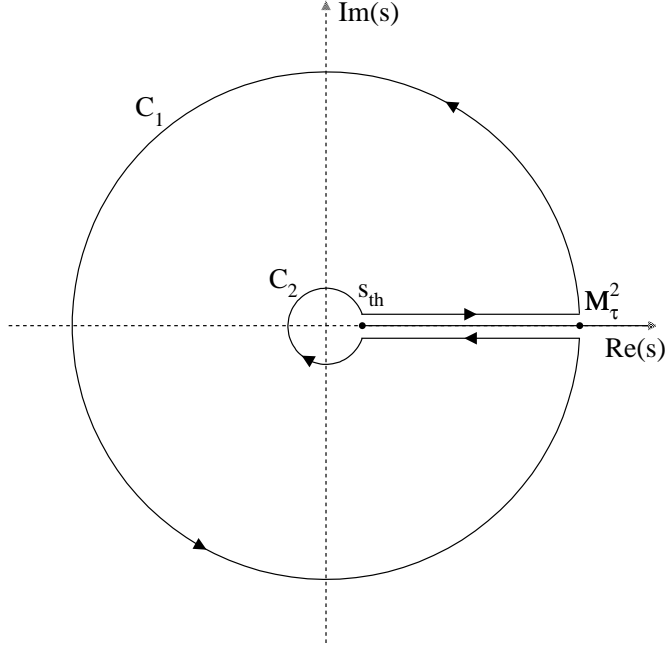


Figure 1: *Integration contour around the circles at $s = M_\tau^2$ and $s = s_{\text{th}}$.*

comes into play: along the small circle placed at the production threshold, $s_{\text{th}} = 4M_\pi^2$ for non-strange ($\bar{u}d$) and $s_{\text{th}} = (M_\pi + M_K)^2$ for strange ($\bar{u}s$) currents, we can use χ PT predictions for the two-point correlators. Using the weight function (5) we adopt the following definition of the moments:

$$R_{\tau,V/A}^{(k,l)} \equiv 12\pi|V_{ud}|^2 S_{\text{EW}} \int_{s_{\text{min}}}^{M_\tau^2} \frac{ds}{M_\tau^2} \left(1 - \frac{s}{M_\tau^2}\right)^{2+k} \left(\frac{s}{M_\tau^2}\right)^l \times \left[\left(1 + 2\frac{s}{M_\tau^2}\right) \text{Im}\Pi_{V/A}^{(0+1)}(s) - 2\frac{s}{M_\tau^2} \text{Im}\Pi_A^{(0)}(s) \right], \quad (6)$$

where $s_{\text{min}} = 0$ for the positive moments¹ ($l \geq 0$) and $s_{\text{min}} = s_{\text{th}}$, which is the continuum threshold, for the inverse moments. According to the relation (4), Eq. (6) reads

$$R_{\tau,V/A}^{(k,l)} = 6\pi i |V_{ud}|^2 S_{\text{EW}} \oint_C \frac{ds}{M_\tau^2} \left(1 - \frac{s}{M_\tau^2}\right)^{2+k} \left(\frac{s}{M_\tau^2}\right)^l \times \left[\left(1 + 2\frac{s}{M_\tau^2}\right) \Pi_{V/A}^{(0+1)}(s) - 2\frac{s}{M_\tau^2} \Pi_A^{(0)}(s) \right], \quad (7)$$

where $C = C_1 + C_2$ for the inverse moments and $C = C_1$ for the positive moments (see Fig. 1).

¹ This is due to the pion pole which is at zero mass in the chiral limit.

Due to the cut of the integral (6) at M_τ^2 , nonperturbative physics parametrized by the short-distance OPE for scalar operators [1, 2, 14] must be considered:

$$\Pi_{V/A}^{(J)}(s) = \sum_{D=0,2,4,\dots} \frac{1}{(-s)^{D/2}} \sum_{\dim \mathcal{O}=D} C_{V/A}^{(J)}(s, \mu^2) \langle \mathcal{O}_{V/A}(\mu^2) \rangle. \quad (8)$$

The parameter μ separates the long-distance nonperturbative effects, absorbed into the vacuum expectation elements $\langle \mathcal{O}_{V/A}(\mu^2) \rangle$, from the short-distance effects which are included in the Wilson coefficients $C_{V/A}(s, \mu^2)$ [1]. We will assume the convergence of the OPE series at the τ mass. This is justified in the light of the success of the analysis performed in Ref. [7] (see Ref. [15] for details). Using the formulae of Refs. [14] and [16] for the nonperturbative power expansion of the correlators, one obtains for the $(V - A)$ case

$$\begin{aligned} \Pi_{\bar{u}d, V-A}^{(0+1)}(-s) &= -\frac{a_s(s) \hat{m}^2(s)}{\pi^2 s} + \left(\frac{8}{3} a_s(s) + \frac{59}{3} a_s^2(s) \right) \frac{\hat{m} \langle \bar{u}u + \bar{d}d \rangle}{s^2} - \frac{16}{7\pi^2} \frac{\hat{m}^4(s)}{s^2} \\ &\quad - 8\pi^2 a_s(\mu^2) \left[1 + \left(\frac{119}{24} - \frac{1}{2} L(s) \right) a_s(\mu^2) \right] \frac{\langle \mathcal{O}_6^1(\mu^2) \rangle}{s^3} \\ &\quad + \frac{2\pi^2}{3} (3 + 4L(s)) a_s^2(\mu^2) \frac{\langle \mathcal{O}_6^2(\mu^2) \rangle}{s^3} + \frac{\langle \mathcal{O}_8 \rangle}{s^4}, \end{aligned} \quad (9)$$

$$\begin{aligned} \Pi_{\bar{u}d, V-A}^{(0)}(-s) &= -\frac{3}{\pi^2} \left[2a_s^{-1}(s) - 5 + \left(-\frac{21373}{2448} + \frac{75}{34} \zeta(3) \right) a_s(s) \right] \frac{\hat{m}^2(s)}{s} - 4\hat{C}(\mu^2) \frac{\hat{m}^2(\mu^2)}{s} \\ &\quad - 2 \frac{\hat{m} \langle \bar{u}u + \bar{d}d \rangle}{s^2} - \frac{1}{7\pi^2} \left(\frac{53}{2} - 12a_s^{-1}(s) \right) \frac{\hat{m}^4(s)}{s^2}, \end{aligned} \quad (10)$$

with $a_s(s) = \alpha_s(s)/\pi$, $L(s) = \log(s/\mu^2)$ and the dimension $D = 6$ operators

$$\begin{aligned} \mathcal{O}_6^1 &\equiv \bar{u} \gamma_\mu \gamma_5 T^a d \bar{d} \gamma^\mu \gamma_5 T^a u - \bar{u} \gamma_\mu T^a d \bar{d} \gamma^\mu T^a u \\ \mathcal{O}_6^2 &\equiv \bar{u} \gamma_\mu \bar{d} \bar{d} \gamma^\mu u - \bar{u} \gamma_\mu \gamma_5 d \bar{d} \gamma^\mu \gamma_5 u, \end{aligned} \quad (11)$$

where the $SU(3)$ generators T^a are normalized so that $\text{tr}(T^a T^b) = \delta^{ab}/2$. We use the average mass $\hat{m} \equiv (m_u + m_d)/2$ in the above equations, *i.e.*, we assume $SU(2)$ symmetry. The constant $\hat{C}(\mu^2)$ depends on the renormalization procedure² and should not affect physical observables. The dimension $D = 0$ contribution is of pure perturbative origin and is degenerate in all-orders of perturbation theory for vector and axial-vector currents. Dimension $D = 2$ mass terms are calculated perturbatively to order α_s^2 which suffices for the light u, d , quarks. The coefficient functions of the dimension $D = 4$ operators for vector and axial-vector currents have been calculated to subleading order in Refs. [17, 18]. Their vacuum expectation values are expressed in terms of the scale invariant gluon and quark condensates. Since the Wilson coefficients of the gluon condensate are symmetric for vector and axial-vector currents, they vanish in

² We will assume a renormalization scheme that preserves chiral symmetry, so that \hat{C} is the same for the vector and axial correlators.

the difference. The expectation values of the dimension $D = 6$ operators (11) obey the inequalities $\langle \mathcal{O}_6^1(\mu^2) \rangle \geq 0$ and $\langle \mathcal{O}_6^2(\mu^2) \rangle \leq 0$, which can be derived from first principles. The corresponding coefficient functions were calculated by the authors of Refs. [19] in the chiral limit for which the $J = 0$ contribution vanishes. For the dimension $D = 8$ operators no such calculations are available in the literature, and we will assume that there is no logarithmic s dependence in leading order α_s . Again, the $J = 0$ contribution vanishes in the chiral limit.

As constraints on the nonperturbative phenomenological operators introduced in Eqs. (9) and (10) from theory alone are scarce, we will benefit from the information provided by the $(V - A)$ spectral moments in order to determine the magnitude of the OPE power terms at M_τ^2 . We therefore perform a combined fit of the IMSR (*i.e.*, $l = -1$) which determines L_{10} , and the $l \geq 0$ moments which adjust the nonperturbative contributions.

3 Chiral Perturbation Theory

The non-strange correlators (2) have been calculated at one-loop level [4, 20] and, most recently, at two-loop level [21, 22] in Standard χ PT. In this paper we stick to the $O(p^4)$ one-loop order for the following two reasons: *i*) the high energy corrections are often more important than the $O(p^6)$ chiral corrections (whose precise estimate has not yet been fully completed [9]) and *ii*) it is important to proceed in the combined analysis order by order in quark masses. On the other hand, we use the generalized version of χ PT (G χ PT) [23], which allows us to investigate the sensitivity of the analysis to the variation of the quark condensate and of the quark mass ratio $r = m_s/\hat{m}$. The standard χ PT assumes [24] $2\hat{m}\langle\bar{q}q\rangle \simeq -F_\pi^2 M_\pi^2$ and $r \simeq 2M_K^2/M_\pi^2 - 1 \approx 25.9$, whereas G χ PT admits lower values of these two quantities [25, 23]. It is interesting to investigate whether the ALEPH spectral function data are precise enough to have any impact on the on-going debate about the size of $\langle\bar{q}q\rangle$. Anyhow, the alterations of the standard $O(p^4)$ results for non-strange correlators (2) introduced by G χ PT are marginal. They merely concern the symmetry breaking $J = 0$ component of the spectral functions and most of them are actually absorbed into the renormalization of F_π (F_K).

In order to make our analysis as independent of a particular truncation of the χ PT series as possible, we proceed in two steps. First, one defines a phenomenological quantity called L_{10}^{eff} via the contribution of the small circle C_2 (see Fig. 1) to the integral (7) of the chiral combination $V - A$ for $l = -1$. L_{10}^{eff} is then determined in the combined fit of the IMSR and $l \geq 0$ moments. The result of this fit is independent of the χ PT renormalization scale $\mu_{\chi\text{PT}}$. The latter is used in the next step in order to relate L_{10}^{eff} to the quark-mass independent, scale dependent constant $L_{10}^r(\mu_{\chi\text{PT}})$ and finally to other observables (from $\pi \rightarrow e\nu\gamma$ data, $\langle r^2 \rangle_\pi$).

3.1 Non-strange IMSR's

For the Cabibbo-allowed channel we obtain:

$$\Pi_{\bar{u}d,V}^{(0+1)}(s) = 4M_{KK}^r(s) + 8M_{\pi\pi}^r(s) - 4(L_{10}^r + 2H_1^r) , \quad (12)$$

$$\Pi_{\bar{u}d,V}^{(0)}(s) = 0 , \quad (13)$$

$$\Pi_{\bar{u}d,A}^{(0+1)}(s) = -\frac{2F_\pi^2}{s - M_\pi^2} - 4(2H_1^r - L_{10}^r) , \quad (14)$$

$$s\Pi_{\bar{u}d,A}^{(0)}(s) = -\frac{2F_\pi^2 M_\pi^2}{s - M_\pi^2} + 8\hat{m}^2(H_{2,2} - 2B_3) , \quad (15)$$

while, for the strange channel the correlators read

$$\Pi_{\bar{u}s,V}^{(0+1)}(s) = 6M_{K\eta}^r(s) + 6M_{K\pi}^r(s) - 4(L_{10}^r + 2H_1^r) , \quad (16)$$

$$s\Pi_{\bar{u}s,V}^{(0)}(s) = 6(L_{K\eta}(s) + L_{K\pi}(s)) + 2\hat{m}^2(r-1)^2(2B_3 + H_{2,2}) , \quad (17)$$

$$\Pi_{\bar{u}s,A}^{(0+1)}(s) = -\frac{2F_K^2}{s - M_K^2} - 4(2H_1^r - L_{10}^r) , \quad (18)$$

$$s\Pi_{\bar{u}s,A}^{(0)}(s) = -\frac{2F_K^2 M_K^2}{s - M_K^2} + 2\hat{m}^2(r+1)^2(H_{2,2} - 2B_3) , \quad (19)$$

The functions $M_{PP'}^r(s)$ and $L_{PP'}(s)$ are loop integrals, defined, *e.g.*, in Ref. [20]. The superscript r refers to renormalized quantities, which depend on the scale $\mu_{\chi\text{PT}}$. The whole expressions are $\mu_{\chi\text{PT}}$ independent. $H_{2,2}$ and B_3 are found to be finite, in agreement with [26], and do not need renormalization. H_1^r and $H_{2,2}$ are coefficients of contact terms of the sources. They are counterterms needed to renormalize the ultraviolet divergences of the Green functions and do not appear in physical observables. Our aim is to determine L_{10} : therefore we will consider the difference between the vector and the axial-vector correlators for which the constant H_1 disappears. Correspondingly, as already pointed out, we will not need the perturbative expressions which are identical for vector and axial-vector cases. As for the constant $H_{2,2}$ which multiplies the term

$$\langle D_\mu \chi^\dagger D^\mu \chi \rangle$$

of the $\mathcal{L}_{(2,2)}$ chiral lagrangian³, it always appears in the same combination with $\hat{C}(\mu^2)$, in such a way that the ambiguities cancel out. We thus define a $\hat{H}_{2,2}$, in which the constant $\hat{C}(M_\tau^2)$ is absorbed. What is new at this order with respect to $S\chi\text{PT}$ is the appearance of the constant B_3 which multiplies the term

$$\langle U^\dagger D_\mu \chi U^\dagger D_\mu \chi + h.c. \rangle$$

³ $\mathcal{L}_{(n,m)}$ collects terms in the chiral lagrangian with n covariant derivatives and m powers of quark masses. In the same notation the H_1 constant introduced by Gasser and Leutwyler [20] would become $H_{4,0}$.

of the $\mathcal{L}_{(2,2)}$ lagrangian. As can be seen from its form it is difficult to find a process in which B_3 would contribute directly. It will contribute to off-shell vertices involving Goldstone bosons.

The non-strange IMSR's corresponding to $l = -1$ and $k = 0, 1$ read:

$$\begin{aligned}
& \frac{1}{|V_{ud}|^2 S_{\text{EW}}} R_{\tau, V-A}^{(0,-1)} \\
&= -96\pi^2 L_{10}^{\text{eff}} + 24\pi^2 \frac{F_\pi^2 M_\pi^2}{M_\tau^4} \\
&+ \frac{144}{M_\tau^2} \hat{m}^2(M_\tau^2) \left[\frac{1}{a_s(M_\tau^2)} - \frac{23}{8} + \left(\frac{\pi^2}{12} - \frac{36061}{4896} + \frac{75}{34} \zeta(3) \right) a_s(M_\tau^2) \right] \\
&+ \frac{96}{M_\tau^4} \pi^2 \hat{m} \langle \bar{d}d + \bar{u}u \rangle \left[1 + a_s(M_\tau^2) + \frac{17}{2} a_s^2(M_\tau^2) \right] - \frac{576}{7M_\tau^4} \hat{m}^4(M_\tau^2) \left[\frac{1}{a_s(M_\tau^2)} - \frac{29}{24} \right] \\
&- \frac{192\pi^4}{M_\tau^6} a_s(\mu^2) \left[1 + \left(\frac{103}{24} - \frac{1}{2} L(M_\tau^2) \right) a_s(\mu^2) \right] \langle \mathcal{O}_6^1(\mu^2) \rangle \\
&+ \frac{400\pi^4}{3M_\tau^6} a_s^2(\mu^2) \left(1 + \frac{12}{25} L(M_\tau^2) \right) \langle \mathcal{O}_6^2(\mu^2) \rangle, \tag{20}
\end{aligned}$$

$$\begin{aligned}
& \frac{1}{|V_{ud}|^2 S_{\text{EW}}} R_{\tau, V-A}^{(1,-1)} \\
&= -96\pi^2 L_{10}^{\text{eff}} - 24\pi^2 \left(\frac{F_\pi^2}{M_\tau^2} - 3 \frac{F_\pi^2 M_\pi^2}{M_\tau^4} + \frac{F_\pi^2 M_\pi^4}{M_\tau^6} \right) \\
&+ \frac{144}{M_\tau^2} \hat{m}^2(M_\tau^2) \left[\frac{1}{a_s(M_\tau^2)} - \frac{71}{24} + \left(\frac{\pi^2}{12} - \frac{39461}{4896} + \frac{75}{34} \zeta(3) \right) a_s(M_\tau^2) \right] \\
&+ \frac{144}{M_\tau^4} \pi^2 \hat{m} \langle \bar{d}d + \bar{u}u \rangle \left[1 + \frac{2}{3} a_s(M_\tau^2) + \frac{43}{6} a_s^2(M_\tau^2) \right] - \frac{864}{7M_\tau^4} \hat{m}^4(M_\tau^2) \left[\frac{1}{a_s(M_\tau^2)} - \frac{2}{3} \right] \\
&- \frac{480\pi^4}{M_\tau^6} a_s(\mu^2) \left[1 + \left(\frac{581}{120} - \frac{1}{2} L(M_\tau^2) \right) a_s(\mu^2) \right] \langle \mathcal{O}_6^1(\mu^2) \rangle \\
&+ \frac{472\pi^4}{3M_\tau^6} a_s^2(\mu^2) \left(1 + \frac{60}{59} L(M_\tau^2) \right) \langle \mathcal{O}_6^2(\mu^2) \rangle + 24\pi^2 \frac{\langle \mathcal{O}_8 \rangle}{M_\tau^8}, \tag{21}
\end{aligned}$$

where we have defined

$$\begin{aligned}
-8L_{10}^{\text{eff}} &= \lim_{s \rightarrow 0} \left\{ \left(1 + \frac{2s}{M_\tau^2} \right) \Pi_{\bar{u}d, V-A}^{(0+1)}(s) - \frac{2s}{M_\tau^2} \Pi_{\bar{u}d, V-A}^{(0)}(s) - \frac{2F_\pi^2}{s - M_\pi^2} - 4 \frac{F_\pi^2}{M_\tau^2} \right\} \\
&+ 8 \frac{\hat{m}^2(M_\tau^2)}{M_\tau^2} \hat{C}(M_\tau^2), \tag{22}
\end{aligned}$$

which is proportional to the contribution of the small circle C_2 to the integral (7), with the pion pole subtracted. This quantity is a well defined observable, the ambiguity in

the two-point function being absorbed by the constant \hat{C} . In the particular case of the one-loop G χ PT calculation, its expansion reads:

$$L_{10}^{\text{eff}} = L_{10}^r(\mu_{\chi\text{PT}}) + \frac{1}{128\pi^2} \left(\log \frac{M_\pi^2}{\mu_{\chi\text{PT}}^2} + 1 \right) + \frac{1}{384\pi^2} \log \frac{M_K^2}{M_\pi^2} + \frac{2\hat{m}^2}{M_\tau^2} (2B_3 - \hat{H}_{2,2}) , \quad (23)$$

which is independent of $\mu_{\chi\text{PT}}$. Unless stated otherwise all condensates, quark masses and χ PT constants in the above expressions are evaluated at QCD renormalization scale $\mu_{\text{QCD}} = M_\tau$, while the product of the light quark mass and the scalar quark operator, $\hat{m}\langle\bar{d}d+\bar{u}u\rangle$, is scale invariant. Taking the difference of Eq. (20) and (21) and subtracting the contribution from the pion pole recovers the expression for $R_{\tau,V-A} = R_{\tau,V-A}^{(0,0)}$ given in [14]. Due to the strong intrinsic correlations of 98% between the IMSR's defined above only one IMSR is used as input to the combined fit. We find it convenient to use the moment $k = 1, l = -1$ (Eq. (21)) because its experimental value is known with a 30% better precision which is due to the additional $(1 - s/M_\tau^2)$ suppression of the less accurate high energy tail of the $(V - A)$ spectral function.

3.2 Strange IMSR

Analogous IMSR's with $l = -2$ would require the two-loop results for the correlators (2), because quark-mass independent terms from the $\mathcal{L}_{(6,0)}$ lagrangian would give rise to new contributions which are not *a priori* small. However, if we consider the difference between the strange and non-strange $(V + A)$ moments these terms cancel out because of the $SU(3)$ symmetry. Of course there will be the two-loop corrections to the terms already present in the one-loop results, but these are subleading. Therefore, we can write a particular combination of inverse moments which does not contain any unknown low-energy constant. An example of such a combination is $4R_{\tau,V+A}^{(1,-1)} + R_{\tau,V+A}^{(2,-2)}$, so that the strange IMSR takes the form:

$$\begin{aligned} & \frac{1}{S_{\text{EW}}} \left[\frac{1}{|V_{us}|^2} (4R_{\tau,S}^{1,-1} + R_{\tau,S}^{2,-2}) - \frac{1}{|V_{ud}|^2} (4R_{\tau,V+A}^{1,-1} + R_{\tau,V+A}^{2,-2}) \right] \\ &= 12\pi^2 \left\{ 4M_\tau^2 \left[\frac{3}{2} (M_{K\eta}^{r'}(0) + M_{K\pi}^{r'}(0)) - M_{KK}^{r'}(0) - 2M_{\pi\pi}^{r'}(0) \right] \right. \\ & \quad + 12 (M_{K\eta}^r(0) + M_{K\pi}^r(0)) - 8 (M_{KK}^r(0) + 2M_{\pi\pi}^r(0)) - 12 (L'_{K\eta}(0) + L'_{K\pi}(0)) \\ & \quad + \frac{12}{M_\tau^2} (F_K^2 - F_\pi^2) - \frac{16}{M_\tau^4} (F_K^2 M_K^2 - F_\pi^2 M_\pi^2) + \frac{6}{M_\tau^6} (F_K^2 M_K^4 - F_\pi^2 M_\pi^4) \left. \right\}_{\approx -7.91} \\ & \quad + 180 \frac{\hat{m}^2}{M_\tau^2} (r^2 - 1) \left[1 + \frac{59}{15} a_s(M_\tau^2) \right] \\ & \quad - 192\pi^2 \frac{1}{M_\tau^4} \langle m_s \bar{s}s - \hat{m} \bar{u}u \rangle \left[1 + \frac{1}{2} a_s(M_\tau^2) + \frac{151}{24} a_s^2(M_\tau^2) \right] \\ & \quad + \frac{576}{7} \frac{\hat{m}^4}{M_\tau^4} \left[(r^4 - 1) \frac{1}{a_s(M_\tau^2)} + \frac{215}{48} - \frac{7}{2} r^2 - \frac{47}{48} r^4 \right] \end{aligned}$$

$$+ \frac{156\pi^2}{M_\tau^6} \langle \mathcal{O}_6^{(\Delta S)} \rangle + \frac{72\pi^2}{M_\tau^8} \langle \mathcal{O}_8^{(\Delta S)} \rangle , \quad (24)$$

where -7.91 is the value of the χ PT contribution, using the π^0 mass and the QCD K^+ mass (*i.e.*, without electromagnetism). We have neglected all logarithmic s dependence in the dimension $D = 6$ and $D = 8$ operators $\mathcal{O}_6^{(\Delta S)}$ and $\mathcal{O}_8^{(\Delta S)}$. The latter are expected to be suppressed because, in contrast to the non-strange \mathcal{O}_6 and \mathcal{O}_8 , they vanish in the chiral limit. Data for the inclusive vector plus axial-vector strange spectral function from τ decays are not available at present. Such data could provide information on the size of the quark condensate, which could represent up to 10% of the χ PT contribution to the r.h.s. of Eq. (24).

4 Theoretical parameters and uncertainties

When fitting the theoretical prediction of the $R_{\tau,V-A}^{(k,l)}$ moments to data, theoretical as well as experimental uncertainties and the correlations of these between the (k, l) moments must be considered. The masses of the light quarks are parametrized using the mass ratio $r = m_s/\hat{m}$ of which the central value is set to the S χ PT value of 26. A lower limit is found at $r \geq r_{\text{limit}} = 2(M_K/M_\pi) - 1 \approx 6.1$ (while $r_{\text{limit}} \approx 8.2$ when including higher orders [27]) which determines the range

$$8 < r < \infty .$$

The average light quark mass is then obtained via $\hat{m} = m_s/r$ where we use for the strange quark mass $m_s(M_\tau) = 172 \text{ MeV}/c^2$ [28]. This parametrization makes it possible to use the theoretical correlation between \hat{m} and the quark condensate, which to leading order in quark masses is given by the generalized Gell-Mann-Oakes-Renner relation [25, 23]:

$$\hat{m} \langle \bar{u}u + \bar{d}d \rangle \simeq -F_\pi^2 M_\pi^2 \frac{(r - r_1)(r + r_1 + 2)}{r^2 - 1} , \quad (25)$$

where $r_1 \simeq 2(M_K/M_\pi) - 1$. For the standard value $r = 25.9$, Eq. (25) becomes the usual PCAC relation $\hat{m} \langle \bar{u}u + \bar{d}d \rangle = -F_\pi^2 M_\pi^2$. Corrections to Eq. (25) are expected to be small in the whole range of r so that we assume a relative uncertainty of 10%. We will comment in Section 6 on the sensitivity of the data with respect to the r ratio. Theoretical uncertainties are introduced from the strong coupling constant where, in order to be uncorrelated to the τ data used in this analysis, we rely on the result from the global electroweak fit found recently to be [29, 30]

$$\alpha_s(M_Z^2) = 0.1198 \pm 0.0031 .$$

Uncertainties from the OPE separation scale μ are evaluated by varying μ from 1.3 GeV to 2.3 GeV, while in the fit we choose $\mu = M_\tau$ so that the logarithmic scale dependence of the dimension $D = 6$ terms vanishes after the contour integration. Additional small uncertainties stem from the pion decay constant, $F_\pi = (92.4 \pm 0.2) \text{ MeV}$,

taken from Ref. [31] and the overall correction factor for electroweak radiation, $S_{\text{EW}} = 1.0194$, obtained in Ref. [32], with an estimated error of $\Delta S_{\text{EW}} = 0.0040$ according to Ref. [33].

An overview of the associated uncertainties in the theoretical prediction of the moments is given in Table 1. The moment errors from the α_s uncertainty depend on the central input values of the nonperturbative operators. The numbers given in the fourth line of Table 1 correspond to the fit values, Eqs. (30)–(31), which have been obtained in an iterative procedure.

5 Spectral Functions from hadronic τ decays

The ALEPH Collaboration measured the inclusive invariant mass-squared spectra of vector and axial-vector hadronic τ decays and provided the corresponding bin-to-bin covariance matrices [6, 7]. The mass distributions naturally contain the kinematic factor of Eq. (6) so that the measured spectral moments read

$$R_{\tau, V-A}^{(k,l)} = \int_0^{M_\tau^2} ds \left(1 - \frac{s}{M_\tau^2}\right)^k \left(\frac{s}{M_\tau^2}\right)^l \left[B_V \frac{dN_V}{N_V ds} - B_A \frac{dN_A}{N_A ds} \right] \frac{1}{B_e}, \quad (26)$$

with the normalized invariant mass-squared spectra $(1/N_{V/A})(dN_{V/A}/ds)$ of vector and axial-vector final states, the electronic branching ratio (using universality) [31, 7], $B_e = (17.794 \pm 0.045)\%$, and the inclusive branching ratios [7], $B_V = (31.58 \pm 0.29)\%$, $B_A = (30.56 \pm 0.30)\%$, as well as their difference, $B_{V-A} = (1.02 \pm 0.58)\%$. Due to anticorrelations between vector and axial-vector final states, especially for the $K\bar{K}\pi$ modes where the vector and axial-vector parts are unknown, the error of the difference is larger than the quadratic sum of the errors on V and A . Figure 2 shows the $(V - A)$ mass-squared distribution, which is the integrand of Eq. (26) for zero moments, $k = l = 0$. With increasing masses it is dominated by the ρ (V), a_1 (A) and the $\rho(1450)$, $\omega\pi$ (V) resonance contributions which create the oscillating behaviour. Table 1 and 2 give the experimental values and uncertainties for the IMSR $R_{\tau, V-A}$ and the $k = 1, l = 0, \dots, 3$ moments as well as their correlations which are computed analytically from the contraction of the derivatives of the moments with the covariance matrices of the respective normalized invariant mass-squared spectra.

Based on isospin invariance, the conserved vector current hypothesis (CVC) relates vector hadronic τ spectral functions to isovector cross section measurements of the reaction $e^+e^- \rightarrow$ hadrons. There exist precise data on the low energy, time-like pion form factor-squared $|F_\pi(s)|^2$ measured by the NA7 Collaboration [34]. Using the CVC relation

$$v_{1, \pi^- \pi^0}(s) = \frac{1}{12} \left(1 - \frac{4M_\pi^2}{s}\right)^{3/2} |F_\pi^{I=1}(s)|^2, \quad (27)$$

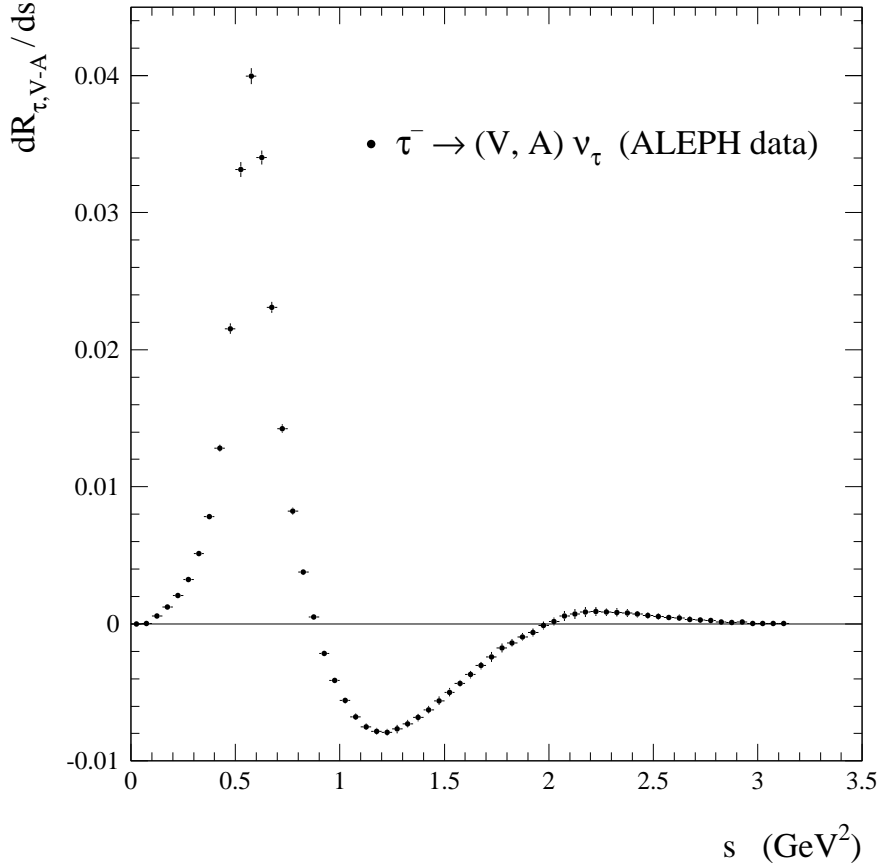


Figure 2: *Vector minus axial-vector ($V - A$) invariant mass-squared distribution measured by ALEPH [7].*

one can include the additional data in order to improve the precision of the moments (26), in particular for the IMSR in which the low-energy region is emphasized. Figure 3 shows the vector spectral function from τ data (three bins) together with the NA7 measurements for energy-squared $s \leq 0.2 \text{ GeV}^2$. In addition, we give the result when fitting both data sets using the parametrization

$$F_\pi(s) = 1 + \frac{1}{6} \langle r^2 \rangle_\pi s + As^2 + Bs^3, \quad (28)$$

for the pion form factor. Using analyticity, the pion charge radius-squared, $\langle r^2 \rangle_\pi = (0.439 \pm 0.008) \text{ fm}^2$, is taken from an analysis of space-like data [35]. We obtain the fit results $A = -(7.5 \pm 1.1) \text{ GeV}^{-4}$ and $B = (62.5 \pm 6.4) \text{ GeV}^{-4}$ with $\chi^2 = 0.6$ for 5 degrees of freedom. The correlation between A and B is absorbed in the diagonal errors given, so that both quantities can be handled as being uncorrelated. Replacing for the above energy interval $4M_\pi^2 \leq s \leq 0.2 \text{ GeV}^2$ the pure τ data by a combination of τ and e^+e^- data represented by the analytical expressions (27) and (28), we obtain the

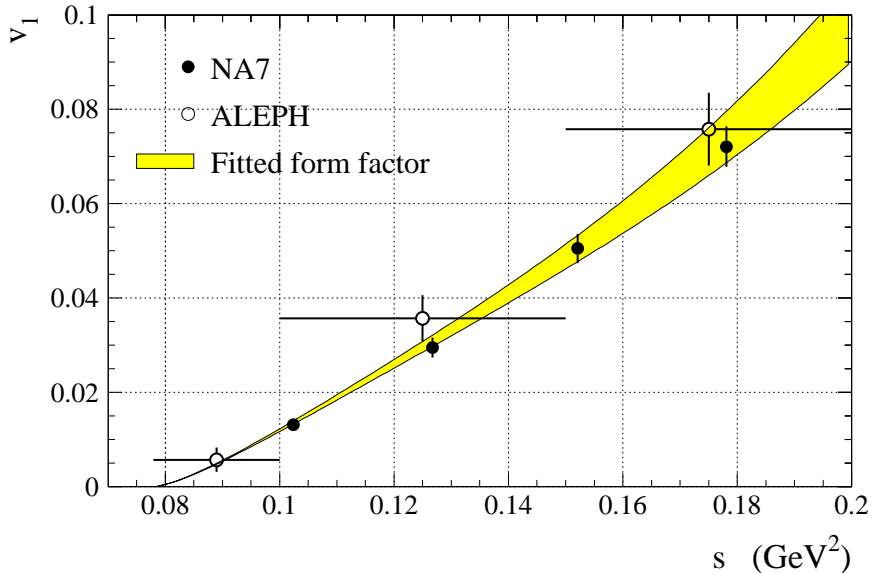


Figure 3: *Low energy vector spectral functions from τ decays and, via CVC, from $e^+e^- \rightarrow \pi^+\pi^-$ data measured by NA7 [34].*

results given in the third and fourth line of Table 1. A small improvement in precision of 11% is observed for the IMSR.

The spectral information is used to fit simultaneously the low-energy quantity L_{10}^{eff} and the nonperturbative phenomenological operators. For dimension $D = 6$ we will neglect the contribution of \mathcal{O}_6^2 , which is suppressed by α_s^2 and, furthermore, is suppressed relatively to \mathcal{O}_6^1 in the large N_c limit. Therefore we will simply keep $\mathcal{O}_6 = \mathcal{O}_6^1(M_\tau^2)$ and the \mathcal{O}_8 operator of dimension $D = 8$.

6 Results of the fit

The fit minimizes the χ^2 of the differences between measured and fitted quantities contracted with the inverse of the sum of the experimental and theoretical covariance matrices taken from Table 2. The results of the fit are for L_{10}^{eff} :

$$L_{10}^{\text{eff}} = -(6.36 \pm 0.09_{\text{exp}} \pm 0.14_{\text{theo}} \pm 0.07_{\text{fit}} \pm 0.06_{\text{OPE}}) \times 10^{-3}, \quad (29)$$

and for the nonperturbative operators:

$$\langle \mathcal{O}_6 \rangle = (5.0 \pm 0.5_{\text{exp}} \pm 0.4_{\text{theo}} \pm 0.2_{\text{fit}} \pm 1.1_{\text{OPE}}) \times 10^{-4} \text{ GeV}^6, \quad (30)$$

$$\langle \mathcal{O}_8 \rangle = (8.7 \pm 1.0_{\text{exp}} \pm 0.1_{\text{theo}} \pm 0.6_{\text{fit}} \pm 2.1_{\text{OPE}}) \times 10^{-3} \text{ GeV}^8, \quad (31)$$

$(k, l) \longrightarrow$	(1, -1)	(0, 0)	(1, 0)	(1, 1)	(1, 2)	(1, 3)
$R_{\tau, V-A}^{(k,l)}$ (ALEPH)	5.16	0.055	0.038	0.047	-0.0164	-0.0126
$\Delta^{\text{exp}} R_{\tau, V-A}^{(k,l)}$	0.09	0.031	0.017	0.006	0.0035	0.0023
$R_{\tau, V-A}^{(k,l)}$ (ALEPH + NA7)	5.13	0.055	0.037	0.047	-0.0164	-0.0126
$\Delta^{\text{exp}} R_{\tau, V-A}^{(k,l)}$	0.08	0.031	0.017	0.006	0.0035	0.0023
$\Delta^{\text{theo}} R_{\tau, V-A}^{(k,l)}$ (Δr)	0.12	0.003	0.003	0.001	0.0003	< 0.0001
$\Delta^{\text{theo}} R_{\tau, V-A}^{(k,l)}$ ($\Delta \alpha_s$)	0.02	0.009	0.009	0.002	0.0029	0.0001
$\Delta^{\text{theo}} R_{\tau, V-A}^{(k,l)}$ (ΔS_{EW})	0.02	< 0.001	< 0.001	< 0.001	0.0001	< 0.0001
$\Delta^{\text{theo}} R_{\tau, V-A}^{(k,l)}$ ($\Delta \mu_{\text{OPE}}$)	< 0.01	0.005	0.005	0.002	0.0018	< 0.0001
$\Delta^{\text{theo}} R_{\tau, V-A}^{(k,l)}$ ($\Delta \langle \bar{q}q \rangle$)	< 0.01	< 0.001	< 0.001	< 0.001	< 0.0001	< 0.0001
$\Delta^{\text{theo}} R_{\tau, V-A}^{(k,l)}$ (ΔF_π)	< 0.01	< 0.001	< 0.001	< 0.001	< 0.0001	< 0.0001
$R_{\tau, V-A}^{(k,l)}$ (Theory fitted)	5.13	0.061	0.032	0.053	-0.0148	-0.0098

Table 1: Measured spectral Moments of vector (V) minus axial-vector (A) using τ data only (ALEPH) and using $\tau + e^+e^-$ data (ALEPH + NA7). The quoted errors account for the total experimental uncertainties including statistical and systematic effects as well as the theoretical uncertainties according to Section 4. The last line gives the fitted theoretical moments using the parameters given in Eqs. (29)–(31).

(k, l)	(1, -1)	(0, 0)	(1, 0)	(1, 1)	(1, 2)	(1, 3)
(1, -1)	1	0.46	0.61	0.40	0.26	0.13
(0, 0)	–	1	0.89	0.97	0.84	0.80
(1, 0)	–	–	1	0.88	0.74	0.45
(1, 1)	–	–	–	1	0.89	0.78
(1, 2)	–	–	–	–	1	0.76

Table 2: Sum of experimental and theoretical correlations between the moments $R_{\tau, V-A}^{(k,l)}$.

	L_{10}	$\langle \mathcal{O}_6 \rangle$	$\langle \mathcal{O}_8 \rangle$
L_{10}	1	-0.26	0.05
$\langle \mathcal{O}_6 \rangle$	–	1	0.14

Table 3: Correlations between the fitted parameters (29)–(31).

with a χ^2 of 2.5 for 3 degree of freedom. The errors are separated in experimental (first number) and theoretical (second number) parts, and a fit uncertainty (third number) is added. The latter is due to a well known bias when fitting quantities for which correlations are due to normalization uncertainties [36] (here the τ branching ratios) leading systematically to lower values in terms of the normalization of the fitted parametrization. The errors quoted account for the differences between fully correlated and uncorrelated results. The authors of Ref. [7] observed a variation of the results on the nonperturbative operators depending on the weighting of the τ spectral functions used in the actual fit. These variations stem from deviations between data and the OPE approach for the running $R_{\tau,V/A}(s_0 \leq M_\tau^2)$ in the vector and axial-vector channels (visualized in Fig. 17 of Ref. [7]) and from the correlation between the fitted dimension $D = 6$ and $D = 8$ operators. They have been found to be larger than the theoretical and experimental uncertainties. We repeat this study here in order to estimate the corresponding systematic uncertainties for the fitted quantities. The last numbers in Eqs. (29)–(31), denoted as “OPE” errors, give the deviations found. They are small for L_{10}^{eff} and dominant for the nonperturbative operators.

Table 3 gives the correlations between the fitted parameters which are found to be small. Nevertheless, the interpretation of the parameter errors given in Eqs. (29)–(31) as individual errors must be done with care in the presence of non-vanishing correlations. The results can reliably be used when applying the whole expansion (8) which yields Eqs. (20) and (21).

Expressing L_{10}^{eff} of Eq. (29) by means of Eq. (23) at the χ PT renormalization scale $\mu_{\chi\text{PT}} = 770$ MeV, we obtain

$$L_{10}^r(M_\rho) = -(5.13 \pm 0.19) \times 10^{-3} . \quad (32)$$

In deriving the above value the term $2\hat{m}^2(2B_3 - \hat{H}_{2,2})$ in Eq. (23) has been neglected. Naïve dimensional analysis estimates [37] give for the low-energy constants B_3 and $H_{2,2}$ an order of magnitude of 10^{-2} , leading to a contribution which is negligible compared to the theoretical error in Eq. (29). The result (32) is to be compared with the one-loop value of L_{10}^r obtainable from $\pi \rightarrow e\nu\gamma$ decays and $\langle r^2 \rangle_\pi$. The error in the latter has been decreased since the first determination of L_{10}^r in Ref. [20]. Using the value $\langle r^2 \rangle_\pi = (0.439 \pm 0.008) \text{ fm}^2$ [35], one obtains

$$L_9^r(M_\rho) = (6.78 \pm 0.15) \times 10^{-3} , \quad (33)$$

which updates the value of Refs. [20, 38]. The L_{10}^r constant can be determined from the one-loop expression of the axial form factor, F_A , of $\pi \rightarrow e\nu\gamma$ (see Ref. [39] for notations):

$$F_A = \frac{4\sqrt{2} M_\pi}{F_\pi} (L_9 + L_{10}) . \quad (34)$$

Taking the value $F_A = 0.0116 \pm 0.0016$ [31], one obtains

$$L_9 + L_{10} = (1.36 \pm 0.19) \times 10^{-3} , \quad (35)$$

and hence

$$L_{10}^r(M_\rho) = (-5.42 \pm 0.24) \times 10^{-3} . \quad (36)$$

This is the updated value of L_{10} to be compared with our result (32). Note that the quoted errors in Eqs. (32)–(36) do not take into account uncertainties from higher order chiral corrections. A two-loop evaluation for the combination $L_9 + L_{10}$ has been attempted in Ref. [39]. However, this analysis is affected by the controversial question about the value of the $SU(2)$ constant l_2 . Using for example the values of Ref. [40] for the constants l_1 and l_2 on the basis of the two-loop precision $\pi\pi$ scattering phenomenology, we obtain $L_9 + L_{10} = (1.07 \pm 0.19) \times 10^{-3}$ instead of $L_9 + L_{10} = (1.57 \pm 0.15) \times 10^{-3}$ given in Ref. [39].

The total, purely nonperturbative contribution to $R_{\tau,V-A}$ found in the fit, taking into account the correlations between the operators, amounts to

$$R_{\tau,V-A} = 0.061 \pm 0.014 , \quad (37)$$

compared to the measurement $R_{\tau,V-A} = 0.055 \pm 0.031$. The reduced error of the theoretical fit to data compared to the measurement stems from the additional information used in the fit which is obtained from the shape of the spectral functions and the OPE constraint. The result (37) is in good agreement with the value of $R_{\tau,V} - R_{\tau,A} = 0.068$ found in Ref. [7]. This is a non-trivial result keeping in mind the logarithmic s dependence of the dimension $D = 6$ Wilson coefficients used in this analysis compared to the vacuum saturation hypothesis adopted in Ref. [7]. In addition, in Ref. [7], vector and axial-vector were not combined in a simultaneous fit. The smaller systematic error on the nonperturbative parts which is found in this analysis, in particular the reduced uncertainty from the explicit dependence of the moments employed, is due to the reduced correlation between the fitted $D = 6$ and $D = 8$ operators (see Table 3). The dimension $D = 6$ contribution to $R_{\tau,V-A}$ corresponding to our fit result Eq. (30) amounts to $R_{\tau,V-A}^{(D=6)} = 0.071 \pm 0.018$, which is significantly than what one obtains from the vacuum saturation hypothesis [14], $R_{\tau,V-A}^{(D=6)} \simeq 0.97 \times 256\pi^3\alpha_s\langle\bar{q}q\rangle^2/M_\tau^6 \approx 0.012$.

In addition to the test of the OPE by varying the (k, l) moments used to fit L_{10}^{eff} and the nonperturbative operators, we perform fits for variable “ τ masses” $s_0 \leq M_\tau^2$ [7] which provides a direct test of the parameter stability at M_τ^2 . In order to perform such a study one has to replace all τ masses in Eqs. (7), (21) and (26) by s_0 , while the latter must be corrected by the kinematical factor $(1 - s/s_0)(1 + 2s/s_0)/s_0$. The scale invariance of the dimension $D = 6$ operator for variable s_0 is approximately conserved when keeping the scale parameter $\mu = M_\tau$ in Eqs. (9) and (21) unchanged. The dimension $D = 8$ operator is assumed to be scale invariant. Figure 4 shows the fitted observables as a function of s_0 . The horizontal bands give the results at M_τ^2 within one standard deviation. All curves show a convergent behaviour for $s_0 \rightarrow M_\tau^2$. Any deviation from the fitted values for $s_0 > M_\tau^2$ should be covered by the “OPE” errors assigned to the results (29)–(31).

Since we use $G\chi\text{PT}$ formulae in this analysis we have investigated the sensitivity

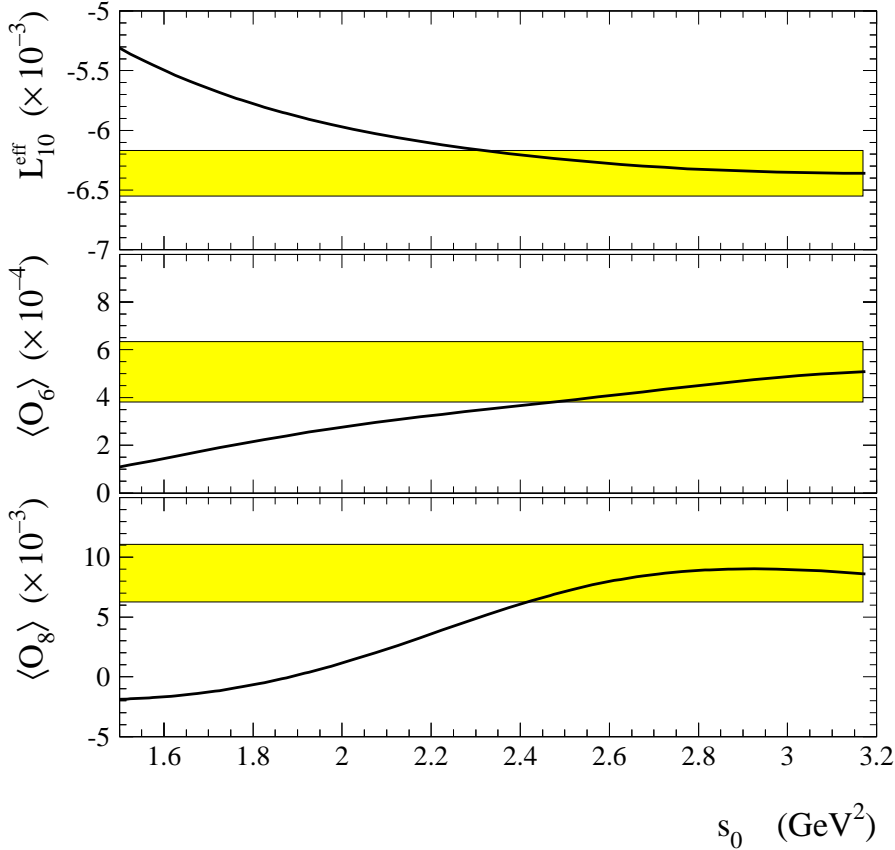


Figure 4: *Fit results for L_{10}^{eff} and the nonperturbative operators as a function of the “ τ mass” s_0 . The bands depict the values (29)–(31) within errors, obtained at M_τ^2 .*

of the $(V - A)$ τ data to a possible constraint on the mass ratio r itself. Clearly a combined fit of L_{10}^{eff} , r and the nonperturbative operators must fail due to the strong correlations of the input variables which reduce the effective degrees of freedom of the fit. Thus, as a test, we may use as input for L_{10}^{eff} and the nonperturbative operators the values (29)–(31) and assume them to be perfectly known, *e.g.*, from a precise second measurement. Fig. 5 shows the theoretical prediction of the (most sensitive) IMSR moment $R_{\tau, V-A}^{(1,-1)}$ as a function of r within the errors from the other theoretical sources given in Table 1, dominated by the error on α_s . Additionally shown as a horizontal band are the ALEPH data within experimental errors. We conclude that the current experimental precision of the non-strange data does not allow to constrain the light quark masses, *i.e.*, the mass ratio r . In the limit of zero u, d quark masses ($r \rightarrow \infty$) we obtain $R_{\tau, V-A}^{(1,-1)} = 5.11$ which is still within the data band of one experimental and theoretical standard deviation. The sensitivity on r when employing the $l \geq 0$ moments is even worse than with the IMSR.

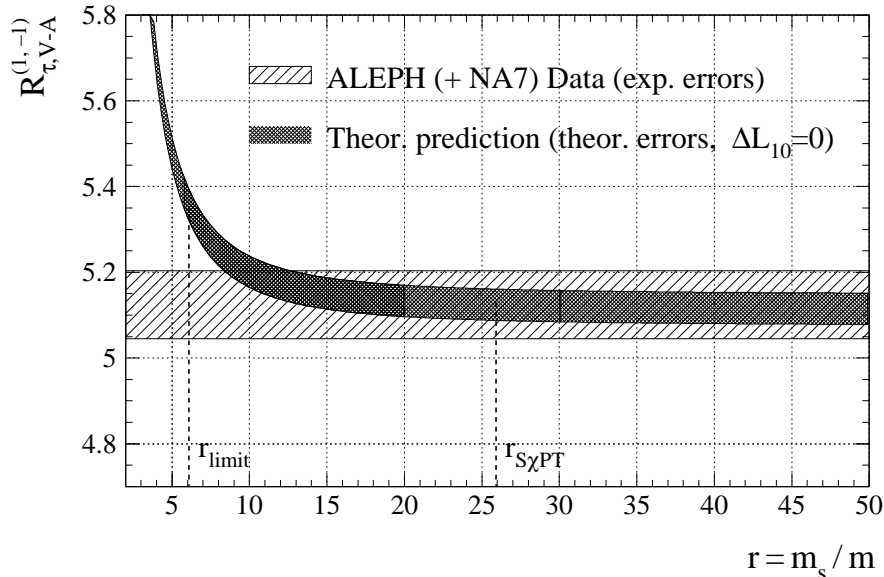


Figure 5: *Theoretical prediction of the IMSR moment $R_{\tau, V-A}^{(1,-1)}$, using $L_{10}^{\text{eff}} = -6.36 \times 10^{-3}$ as fixed input value, versus the mass ratio r . The theoretical uncertainty stems mainly from the error on $\alpha_s(M_\tau^2)$. The dashed band shows the $(V - A)$ data from hadronic τ decays (including low energy e^+e^- vector cross sections) within experimental errors.*

7 Conclusions

This article deals with a combination of finite energy sum rule techniques and Chiral Perturbation Theory (χ PT) low-energy expansion in order to exploit recent ALEPH data on the non-strange τ vector and axial-vector spectral functions with respect to an experimental determination of the χ PT quantity L_{10} . The theoretical predictions of the spectral moments, $R_{\tau, V-A}^{(k,l)}$, of the τ hadronic width involve nonperturbative elements of the Operator Product Expansion when calculating the contour integral at $|s| = M_\tau^2$. In the case of inverse spectral moments ($l < 0$), additional χ PT parameters appear originating from a second contour integral at the $|s| = 4M_\pi^2$ production threshold which subtracts the singularity of the $(s/M_\tau^2)^{-1}$ inverse moment at $s = 0$. A constrained fit of $l < 0$ and $l \geq 0$ spectral moments adjusts simultaneously the parameter L_{10}^{eff} , defined by Eq. (22), and nonperturbative power operators of dimension $D = 6$ and $D = 8$. We obtain $L_{10}^{\text{eff}} = -(6.36 \pm 0.09 \pm 0.16) \times 10^{-3}$, where the first error is of experimental and the second of theoretical origin. The present determination of L_{10}^{eff} is independent of any chiral expansion; in particular, the value obtained here can be directly used in a two-loop analysis: it suffices to include higher order corrections in Eq. (23). Within the one-loop χ PT the above result corresponds to $L_{10}^r(M_\rho) = -(5.13 \pm 0.19) \times 10^{-3}$, in good agreement with the value $L_{10}^r(M_\rho) = -(5.42 \pm 0.24) \times 10^{-3}$ extracted from the one-loop analysis of $\pi \rightarrow e\nu\gamma$ data and $\langle r^2 \rangle_\pi$. This provides a non-trivial test of chiral symmetry underlying χ PT. The total nonperturbative prediction to $R_{\tau, V-A}$

found in the fit, is in agreement with the values of the ALEPH $\alpha_s(M_\tau^2)$ analysis [7]. The stability of the fit results is investigated in performing various fits for “ τ masses” smaller than M_τ . Satisfactory convergence is observed.

References

- [1] K.G. Wilson, *Phys. Rev.* **179** (1969) 1499
- [2] M.A. Shifman, A.L. Vainshtein and V.I. Zakharov, *Nucl. Phys.* **B147** (1979) 385, 448, 519
- [3] S. Weinberg, *Physica* **A96** (1979) 327
- [4] J. Gasser and H. Leutwyler, *Ann. Phys.* **158** (1984) 142
- [5] J.F. Donoghue and E. Golowich, *Phys. Rev.* **D49** (1994) 1513
- [6] ALEPH Collaboration (R. Barate *et al.*), *Z. Phys.* **C76** (1997) 15
- [7] ALEPH Collaboration (R. Barate *et al.*), Report CERN PPE/98-012 (1998), to appear in *The Europ. Phys. J. C*
- [8] T. Das, V.S. Mathur and S. Okubo, *Phys. Rev. Lett.* **19** (1967) 895
- [9] E. Golowich and J. Kambor, preprint UMHEP-447, ZU-TH 30/97, hep-ph/9711256
- [10] F. Le Diberder and A. Pich, *Phys. Lett.* **B289** (1992) 165
- [11] D. Buskulic *et al.* (ALEPH Collaboration), *Phys. Lett.* **B307** (1993) 209
- [12] T. Coan *et al.* (CLEO Collaboration), *Phys. Lett.* **B356** (1995) 580
- [13] E. Golowich and J. Kambor, *Phys. Rev.* **D53** (1996) 2651
- [14] E. Braaten, S. Narison and A. Pich, *Nucl. Phys.* **B373** (1992) 581
- [15] A. Höcker, “*Measurement of the τ spectral functions and applications to QCD*”, Thesis, Report LAL 97-18, Orsay, France (1997)
- [16] K.G. Chetyrkin and A. Kwiatkowski, *Z. Phys.* **C59** (1993) 525
- [17] S.C. Generalis, *J. Phys.* **G15** (1989) L225
- [18] K.G. Chetyrkin, S.G. Gorishny and V.P. Spiridonov, *Phys. Lett.* **B160** (1985) 149
- [19] L.V. Lanin, V.P. Spiridonov and K.G. Chetyrkin, *Yad. Fiz.* **44** (1986) 1372; *Sov. J. Nucl. Phys.* **44** (1986) 892
- [20] J. Gasser and H. Leutwyler, *Nucl. Phys.* **B250** (1985) 465
- [21] E. Golowich and J. Kambor, *Nucl. Phys.* **B447** (1995) 373
- [22] E. Golowich and J. Kambor, preprint ZU-TH-19-97, hep-ph/9710214

- [23] M. Knecht and J. Stern, *The second DAΦNE Physics Handbook, Vol I*, (Eds. L. Maiani, G. Pancheri and N. Paver), INFN, Frascati (1995) 169
- [24] S. Weinberg, “*A Festschrift for I.I. Rabi*”, Eds. L. Motz, New York Academy of Sciences, New York (1977)
- [25] N.H. Fuchs, H. Sazdjian and J. Stern, *Phys. Lett.* **B238** (1990) 380; *Phys. Lett.* **B269** (1991) 183
- [26] M. Knecht, *to be published*
- [27] J. Stern, “*Light Quark Masses and Condensates in QCD*”, Invited plenary talk given at the Workshop on Chiral Dynamics: Theory and Experiment (ChPT97), Mainz, Germany, report IPNO/TH-97-30, hep-ph/9712438
- [28] S. Chen, “*Measurement of τ decays with kaons from ALEPH and m_s determination*”, Talk given at QCD’97, Montpellier, France 1997
- [29] D. Ward, “*Tests of the Standard Model: W mass and WWZ Couplings*”, Talk given at the International Europhysics Conference on High-Energy Physics (HEP 97), Jerusalem, Israel 1997
- [30] M. Davier and A. Höcker, Report LAL 97-85, hep-ph/9711308 (1997), *to appear in Phys. Lett. B*
- [31] R.M. Barnett *et al.* (Particle Data Group), *Phys. Rev.* **D54** (1996) 1
- [32] W.J. Marciano and A. Sirlin, *Phys. Rev. Lett.* **56** (1986) 22; *Phys. Rev. Lett.* **61** (1986) 1815
- [33] R. Alemany, M. Davier and A. Höcker, Report LAL 97-02 (1997), *to appear in The Europ. Phys. J. C*
- [34] NA7 Collaboration (S.R. Amendolia *et al.*), *Phys. Lett.* **B138** (1984) 454
- [35] NA7 Collaboration (S.R. Amendolia *et al.*), *Nucl. Phys.* **B277** (1986) 168
- [36] G. D’Agostini, *Nucl. Inst. Meth.* **A346** (1994) 306
- [37] H. Georgi, *Phys. Lett.* **B298** (1993) 187
- [38] J. Bijnens, G. Ecker and J. Gasser, *The second DAΦNE Physics Handbook, Vol I*, (Eds. L. Maiani, G. Pancheri and N. Paver), INFN, Frascati (1995) 125
- [39] J. Bijnens and P. Talavera, *Nucl. Phys.* **B489** (1997) 387
- [40] L. Girlanda, M. Knecht, B. Moussallam and J. Stern, *Phys. Lett.* **B409** (1997) 461